

Modelling Oriented Macromolecular Assemblies from Low-angle X-ray Fibre Diffraction Data with the Program MOVIE: Insect Flight Muscle as an Example

Hind A. AL-Khayat¹, Liam Hudson¹, Michael K. Reedy², Thomas C. Irving³
and John M. Squire¹

[1] Biological Structure & Function Section, Biomedical Sciences Division, Faculty of Medicine, Imperial College London, London SW7 2AZ, UK

[2] Dept of Cell Biology, Duke University, Durham, NC 27710, USA

[3].BioCAT, Dept. Biological, Chemical and Physical Sciences, Illinois Institute of Technology, Chicago, IL 60616, USA

Received and 3rd March 2004; accepted in revised form 2nd April 2004

ABSTRACT

Many extended biological structures such as actin and myosin filaments, intermediate filaments, microtubules, flagella and so on can form oriented fibrous assemblies which are either naturally occurring, as in muscle or hair, or can be induced to form synthetic fibres. Such structures can yield very rich fibre diffraction patterns. Part of the remit of CCP13 in Fibre Diffraction and Solution Scattering is to strip such diffraction patterns to produce reliable intensity values for the diffraction peaks. However, since such diffraction patterns usually arise from structures with cylindrical symmetry around the preferred long axis, implying that even well-sampled fibre patterns inevitably contain many overlapping diffraction peaks, they cannot be phased in the same way as for protein crystallography and it is necessary to devise modelling strategies to interpret the diffraction patterns. For high-angle diffraction data from highly organised molecular structures (e.g. DNA or cellulose) the program LALS can be used effectively. In the case of low-angle X-ray fibre diffraction patterns we have generated the program MOVIE to take known protein crystal structures and use these in simulated annealing configurational searches to optimise the fit between the observed and calculated diffraction data. Here we describe the rationale behind MOVIE and the steps involved in applying MOVIE to a typical case, namely the analysis of the low-angle X-ray fibre diffraction data from relaxed insect flight muscle recorded on the BioCat beamline at the Argonne APS.

Introduction to Muscle and the Strategy behind MOVIE

Muscle cells (fibres) contain two parallel sets of protein filaments made of myosin and actin respectively (Figure 1(a)). During stretch or shortening, the overlapping myosin and actin filaments each keep virtually constant length as they slide past each other. They change their overlap as the muscle changes length. To perform the sliding motion, myosin heads (crossbridges) projecting out from the myosin filament surface cyclically bind to, bend on, then release, adjacent actin filaments as if they were walking along the actin. The bind-and-bend phase of each cycle is called a powerstroke. The end of the powerstroke, in which myosin heads have already bent and are strongly bound to actin, is called the rigor-like conformation. This conformation has previously been visualised both by electron microscopy and by modelling X-ray diffraction data (e.g. Rayment *et al.*, 1993b; Harford *et al.*, 1996). However, the orientation of the unbound heads in myosin's relaxed initial state or in the first attachment to actin have not been known in detail until recently. Comparing the

positions of the heads in the two states can help to deduce the structural transitions involved in the powerstroke mechanism following muscle activation.

The structure of the myosin head (myosin subfragment 1 or S1) has been determined by protein crystallography (Figure 1(b)). Myosin S1 heads are enzymes (ATPases) which bind and split the energy-giving molecule ATP (adenosine triphosphate) to give the products ADP (adenosine diphosphate) and inorganic phosphate (Pi). The myosin head state that initially attaches to actin in the pre-powerstroke state is M.ADP.Pi, giving AM.ADP.Pi when attached to actin. Force production and movement occur when Pi and then ADP are released from the heads to leave the AM (rigor-like) state. Addition of ATP to AM causes the release of the heads from actin and the resulting M.ATP state rapidly dissociates to M.ADP.Pi once again, leaving the head ready for a further cycle of attachment and movement on actin. The first myosin head shape to be solved by protein crystallography was in the absence of nucleotide, as in the 'rigor' state (Rayment *et al.*, 1993a). Since that time attempts have been made to mimic the head shape in the pre-powerstroke state in protein crystals,

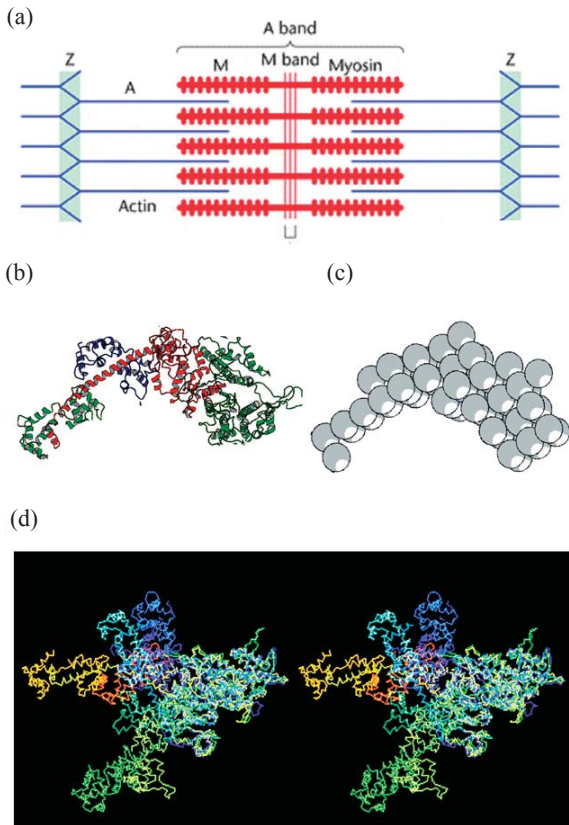


Figure 1. (a) The structure of a striated muscle sarcomere, which extends from Z-band (Z) to Z-band, showing the overlapping actin and myosin filaments and the projections on the myosin filaments in the muscle A-band. (b) The myosin head structure (Rayment *et al.*, 1993a) as downloaded from the PDB database and illustrating the myosin heavy chain (green and red on the right (the catalytic domain) and red on the left (the neck region)). The neck region or lever arm also has the two light chains; the regulatory light chain (green on the left) and essential light chain (blue). The long α -helical part of the heavy chain in red in the core of the light chains region provides the link between the catalytic domain and the rest of the myosin filament which joins at the bottom left hand part of the red helix. The actin-binding face of the myosin head is top right and slightly facing up and out of the page. (c) Representation of (b) in terms of a 59 sphere model. The volume of these spheres, each of radius 8.61 Å, was chosen to express the overall mass of the myosin head, assuming constant protein density within all spheres. (d) Stereo-images of various crystal structures of the myosin head with different nucleotides bound. All are superimposed at the motor catalytic domain on the right, so that the differences between models are expressed by the different positions of the neck regions or lever-arms on the left. Green and pointing slightly towards the viewer is the Rayment *et al.* (1993a,b) chicken skeletal myosin with no nucleotide (i.e. rigor-like); dark blue is the Dominguez *et al.* (1998) chicken smooth muscle myosin in ADP·AlF₄ form; pale blue is our *Lethocerus* model; orange is the Houdusse *et al.* (2000) scallop myosin in Mg·ADP·VO₄ form. The view has the actin filament axis vertical and to the right, with the M-band at the top and Z-band at the bottom.

yielding success with smooth muscle myosin and bound ADP·AlF₄ in the work of Dominguez *et al.* (1998) and with scallop muscle myosin and bound ADP·VO₄ in the work of Houdusse *et al.* (2000). These and other crystallographic studies of myosin have shown that the ATP-binding part of the head, known as the catalytic or motor domain, is relatively constant in shape, at least at low resolution, but that the rest of the head forms a relatively narrow and straight neck region which can change its angle relative to the motor domain

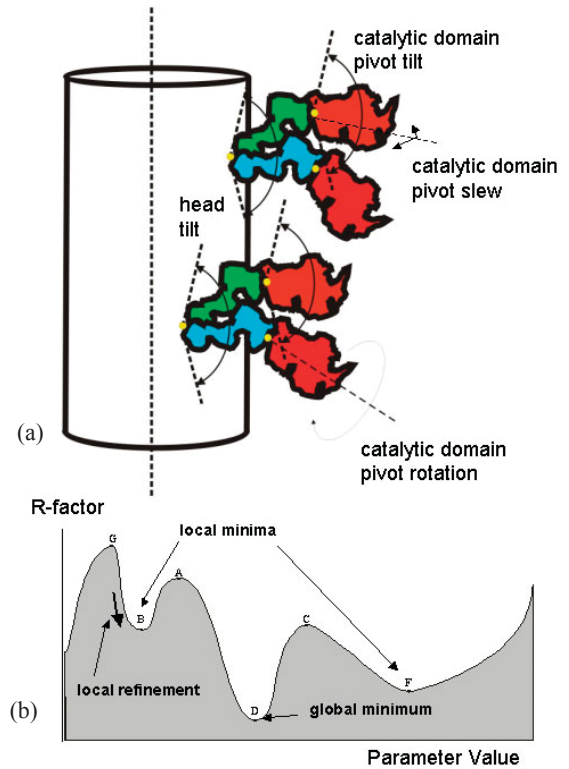


Figure 2. (a) Illustration of pairs of myosin heads on helical tracks on the surface of a roughly cylindrical myosin filament backbone, with the hinge points at the filament surface and between the motor domain and neck region illustrated (yellow circles), together with some of the kinds of parameters which can describe the head shape and position. (b) Illustration of the variation of the R-factor in hypothetical parameter space showing local minima at B and F and a global minimum at D.

depending on the attached nucleotide. Several different head shapes are illustrated in Figure 1(d).

Myosin molecules comprise two of the S1 heads discussed above, each about 16 nm long, on the end of a rod-shaped tail about 150 nm long. The myosin tails or rods pack together to form the shaft of the myosin filaments with the myosin heads in quasi-helical arrays on the filament surface (Figure 2(a)). In resting muscles the heads are often relatively well-ordered on the filament backbones and they give rise to strong diffraction features in low-angle X-ray diffraction patterns (Figure 3). The process of head movement and attachment to actin filaments during muscle contraction clearly disrupts this starting structure and gives rise to new diffraction features. In this paper we are primarily concerned with illustrating the use of the program MOVIE by discussing how to model the myosin filaments in resting insect flight muscle. The problem is that, although we know the geometry and symmetry of the lattice of heads that occurs on the myosin filament surface (and this is different for different muscle types), we do not know the head shape in this state (the heads are probably predominantly in the M·ADP·Pi biochemical state; Hibberd and Trentham, 1986; Xu *et al.*, 1999) and we do not know the arrangement of the two heads of each pair on the filament surface. This is where the program MOVIE comes into play.

What MOVIE does

The problem is as follows, remembering that we are dealing with diffraction features at relatively low resolution. We can define the position of each of the myosin heads in a pair (Figure

2(a)), using the far end of the neck or lever arm away from the motor domain as an origin, in terms of their radius (R) from the filament axis, and in terms of various angles such as the head slew (α) around an axis through the head origin and parallel to the filament long axis, the head tilt (β) in a direction parallel to the filament axis, and the head rotation (θ) about the myosin head's own long axis. In addition, since we do not know the head shape, we can suppose that, with the neck position defined by the angles α , β and θ , the motor domain can rotate relative to the neck region around three further mutually perpendicular axes (motor pivot tilt α_p , motor pivot slew β_p , and motor pivot rotation θ_p). In addition, the two heads in one pair cannot have identical origins on the filament surface, so they need to be offset by two further parameters (their separation H_s and the tilt of the line joining the origins H_t). In the case of insect flight muscle, which is highly ordered in 3-dimensions, the orientation (ϕ) of the whole myosin filament about its own long axis within the muscle unit cell is also an important factor. These parameters are explained in detail in AL-Khayat *et al.* (2003).

The insect flight muscle myosin filament is a relatively simple example of its kind since the myosin head array appears to be purely helical. The filaments have 4-fold rotational symmetry, meaning that there are the heads of four myosin molecules equally spaced in a ring around the myosin filament. Such a ring is known as a 'crown'. Successive crowns along the filament are separated axially by 14.5 nm and by a rotation of 33.75° , giving the filament a true axial repeat after 8×14.5 nm (116 nm). It is therefore enough in the MOVIE program to define the positions of each head in the pair belonging to one molecule and then to assume that all the other heads are related to these first heads purely by applying the helical symmetry of the filament. This means that the diffraction pattern from the filament can be computed using Fourier transforms involving Bessel functions as described elsewhere (Harford and Squire, 1997; Squire, 2000; AL-Khayat *et al.*, 2003).

From the discussion of appropriate parameters above, the insect problem reduces to optimising the value of 13 parameters, assuming that both heads have the same shape (α , β and θ for each of two heads, α_p , β_p , θ_p defining the common head shape, and R , H_s , H_t , ϕ). What we would ideally like to do is to represent the myosin head by its atomic coordinates as in a PDB file and then run a global search routine where every parameter is stepped through a small increment, the diffraction pattern for each parameter combination is checked against the observed pattern and a 'goodness of fit factor, R , is calculated (like the crystallographic R -factor). However, in attempting to do this one soon comes up against a chronic shortage of computing power. The various head parameter angles will range either from -90° to $+90^\circ$ or from -180° to $+180^\circ$ and we would wish to sample these in steps of say 1° or 2° (i.e. 90 to 360 steps for each angle). Other angles such as H_t and ϕ might have smaller ranges, say $\pm 45^\circ$ in steps of 2° for H_t (45 combinations) and say 0° to 12° for ϕ in steps of 1° (13 values). Distances such as R and H_s might have a limited sensible range (say 7 to 10 nm for R and 2 to 5 nm for H_s) and one would want to step these in increments of, say, 0.1 or 0.2 nm (about 15 to 30 steps for each). Even taking the larger step sizes, the number of parameter combinations is at least $(90)^9 \times (15)^2 \times 45 \times 13 = 5.099 \times 10^{22}$. Let us suppose (optimistically) that each parameter

computation and comparison with the observed diffraction data, resulting in a value for the goodness of fit factor R , takes 1 ms. This then means that the whole search will take of the order of 10^{12} years! Even a computer farm and a great deal of parallel computing will not help very much. However, a number of strategies may be invoked to speed things up. First of all one can try to make each individual calculation faster. This can be done by representing the low-resolution shape of the myosin head by a relatively small number of spheres rather than by all the atomic coordinates. We have found that a model involving 59 spheres each of radius 8.61 Å (Figure 1(c)) can adequately represent the myosin head at the resolution we are considering (say 6 nm). In fact the computed diffraction patterns from the sphere model and the PDB model (Figure 1(b)) agree with a correlation coefficient of 0.995 to 6.5 nm resolution. This simplification speeds up the calculation considerably. In fact, for a single MOVIE calculation for only one parameter set takes 1.052 seconds with the full PDB file and 0.054 seconds with the sphere model, and so the search with the sphere model is about 20 times faster than with using the full PDB file. Next we can think of less systematic but faster ways of searching through parameter space to home in on the best parameter set. In fact there are various established approaches to this, such as the Downhill Simplex refinement (Nelder and Mead 1965; Brent, 1973). However, one can imagine being in a local minimum in R space (points B or F in Figure 2(d)) and being taken to the bottom of that minimum by the Downhill Simplex procedure, but then being trapped there, even though the true minimum is elsewhere (point D). A good way to avoid this problem is to use the process of simulated annealing (Kirkpatrick *et al.*, 1983; Kirkpatrick, 1984). This has the effect of allowing the parameters to effectively 'jump around' in parameter space, thus avoiding local minima traps, with the range of the jumping defined by the 'temperature' at which the simulation is running. In successive cycles this 'temperature' can be reduced until a stable set of parameters is obtained. Subsequent local refinement by a Downhill Simplex run will then, it is hoped, take the parameters to the bottom of the global minimum well (D in Figure 2(d)). As described below, application of such a simulated annealing approach to the muscle problem using the program MOVIE has already yielded excellent results (Hudson *et al.*, 1997; Squire *et al.*, 1998; AL-Khayat *et al.*, 2003).

Getting good intensity data using LSQINT

The diffraction pattern in Figure 3 was stripped and analysed as illustrated in Figure 4, where Figure 4(a) is the quadrant-folded version of Figure 3. Analysis of this pattern presented a number of problems. Firstly the pattern contains mixed contributions from actin filaments as well as myosin filaments. Because the helical symmetry and repeats in both filaments are known, we knew that layer-lines with spacings common to both filaments (2320 Å) would have contributions from myosin and actin on the same layer-line (e.g. the 6th order of 2320 Å at 38.7 nm). It was, therefore, necessary to separate out the few layer-lines coming solely from myosin and to use these in our analysis. Secondly, because we did not need either the equator or the meridian to do the analysis, we could mask off those regions of the diffraction pattern as in Figure 4(b). Finally, in trying to use LSQINT, it was noted that, for example, the 6th layer-line at a 38.7 nm spacing, which has strong contributions from the actin filaments, had different peak shapes from the layer-lines arising solely from the myosin filaments. However, Figure 4(c) shows

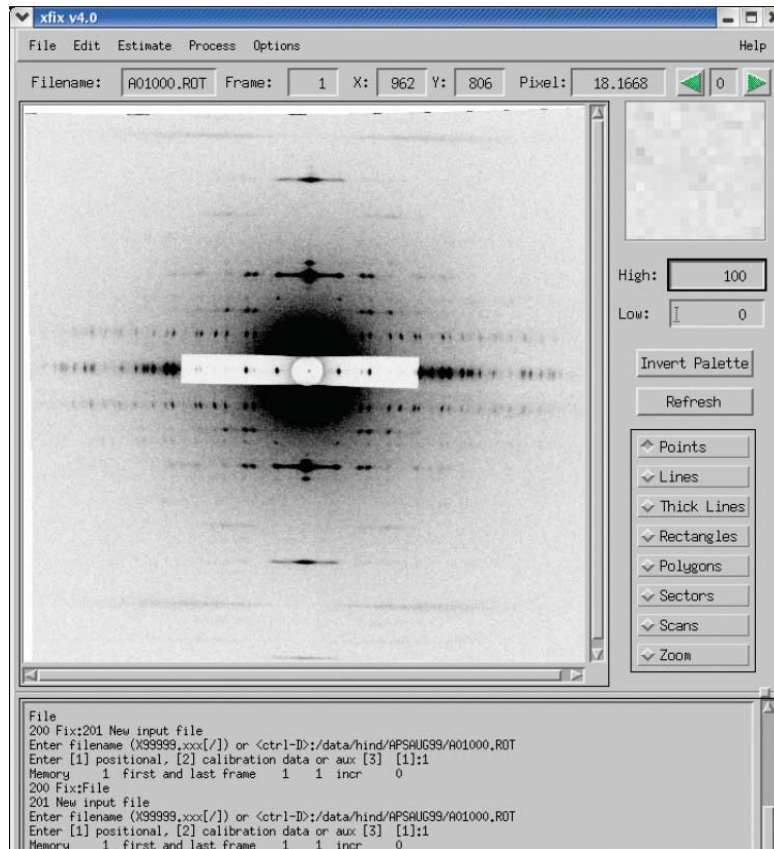


Figure 3. A low-angle X-ray diffraction pattern from relaxed flight muscle fibres [dorsal longitudinal muscles (DLM)] from the giant waterbug (*Lethocerus indicus*) recorded using X-rays of $\lambda = 1.033 \text{ \AA}$ on the BioCAT beamline 18-ID at the APS using the small angle camera described by Irving T.C. *et al.*, (2000) at a 1960 mm specimen-detector distance and a CCD detector (Reedy, M.K. *et al.*, 2000). A strip of Al sheet metal about 0.4 mm thick was positioned over the CCD along the equator, attenuating the strongest equatorial spots to about 0.01 and thereby avoiding a readout artefact in the CCD images. 100 ms exposures using 90% beam attenuation routinely gave good patterns from fibre bundles 250-350 μm in diameter. About ten patterns approaching this quality were obtained, but none quite matched its orientation and spot-sharpness, so this pattern was used for definitive final analysis. Here the pattern is shown contained in the window of the CCP13 XFIX program.

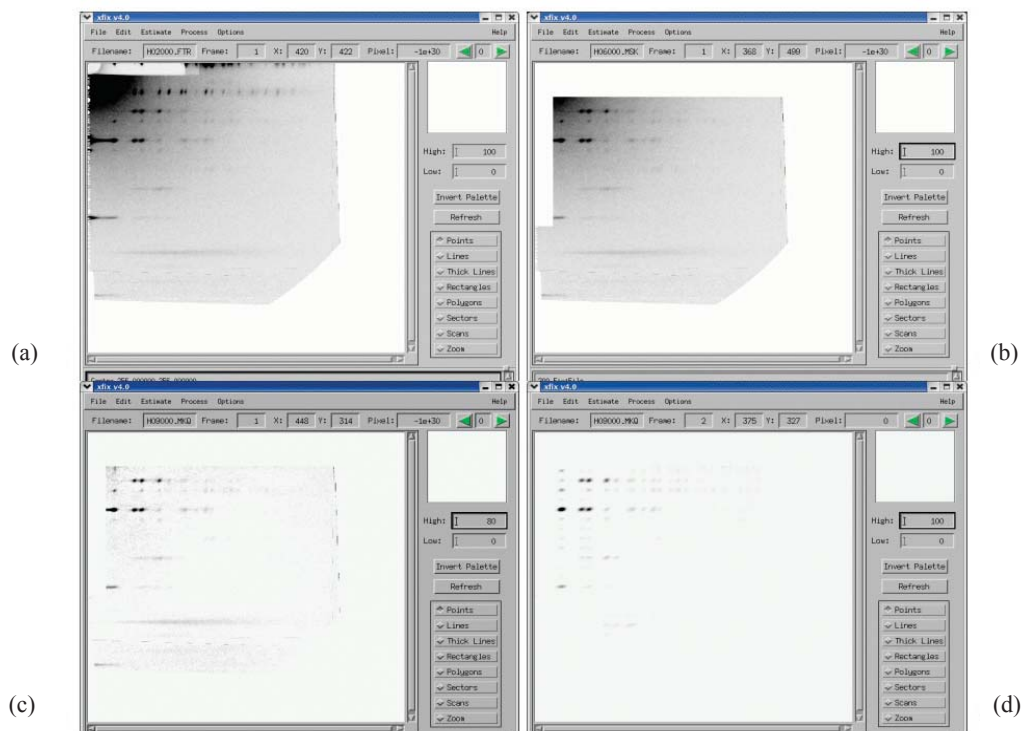


Figure 4. (a) Average of four quadrants of Figure 3 after converting into reciprocal space in FTOREC, (b) same as in (a) but with a mask on the equator, the 38.7 nm layer line and the meridian, (c) LSQINT output of fitting the pattern shown in (b) after subtracting the fitted background, (d) fitted intensity peaks in (c) produced by LSQINT and as used in the modelling studies of this paper. All these patterns are shown contained in the window of the CCP13 XFIX program.

the pattern in Figure 4(b) after fitting and subtracting a suitable background, and Figure 4(d) shows the LSQINT fit to the remaining Bragg peaks. The original pattern had over 468 Bragg reflections, of which over 65 were strong and exclusively from the myosin filaments to a resolution of $1/65 \text{ \AA}^{-1}$. These 65 intensities were then modelled as described above using the known myosin head shape represented as spheres, a hinge between the motor (catalytic) domain and the light chain-binding (neck) region (lever arm), and a simulated annealing model search procedure.

Running the MOVIE program

MOVIE is a program originally written by J. M. Squire in Fortran 77 (it was originally called MUSCLE3D). It was converted to the C language and the simulated annealing parameter search procedure was added by L. Hudson (Hudson, 1996). It was later modified by H. A. AL-Khayat. It runs on a UNIX shell using LINUX or ALPHA workstations.

The program is centred around a command line interface which works by the user inputting keywords and numerical values/character strings to set up the starting conditions. The keywords may be split into three distinct types: Single commands: these keywords can either be ENABLED or DISABLED. They always default to DISABLED (Figure 5a, with all default model parameters set to zero) and can be ENABLED when selected (e.g. myosin, actin, simplex, anneal, view etc). Simple commands: these keywords are always followed by another single parameter which can either be an integer, floating point or a character string (e.g. cell 523.44, mrepeat 1167.41, filaments 1, numreps 3, mcrowns 8). Complex commands: these keywords have a range of sub-keywords associated with them. Each sub-keyword is in effect a simple command mentioned above, each with its own number or character string associated with it (e.g. mslew head 1 start -65.03 scale 2.0). All these commands can be in lower or upper case. MOVIE has about 120 keywords and a complete list of all the commands plus their descriptions can be obtained by pressing the 'RETURN' key while within MOVIE.

Under normal usage, it is easier to create a template file which contains a list of commands and model parameter values. This file can be parsed via the 'load' keyword. An example template file is shown in Figure 5(b) for running a simulated annealing search. The processing then starts with the command 'run'. By default, the program always outputs its results to the terminal screen (Figure 6), this can be re-directed to a named file via the keyword 'outputfile'. This enables the user to view the output file when the user is not necessarily sitting at the terminal. All commands inputted to the program are recorded along with any error messages in a log file called 'Movie.log'. This file can be analysed if a process does not produce the expected results.

A typical template file created to be used in MOVIE for a simplex search run for local minimisation and refinement is shown in Figure 7(a).

MOVIE has three output forms for the viewing mode: (i) a PDB atomic coordinates format, (ii) a sphere representation, (iii) DCAD, format which can be viewed with a WINDOWS software package called DESIGNCAD3D, and finally (iv) a 3D electron density map.

A typical template file to be used in creating an output PDB file for the coordinates of a model is shown in Figure 7(b). The second form of output from MOVIE, in which model parameters are output in cartesian coordinates for the positions of the centres and radii of spheres, we can use AVS for displaying the model in 3D space. The template file used in creating an output ascii file for the cartesian coordinates of a sphere representation of the model is shown in Figure 8(a). For the output file of this to be read in AVS, an AVS field file of the form shown in Figure 8(b) is also required.

The result of the PDB viewing mode is shown in Figure 9(a) displayed in RASMOL, showing one crown in end-on view (left) and slightly tilted side view (right) for the best model. The PDB file can also be viewed using any other crystallographic software, including FRODO, GRASP, O and PDBVIEWER. Figure 9(b) is the same as in Figure 9(a) but in the sphere representation viewed in AVS of the end-on view (left) and slightly tilted side view (right). It clearly shows the close similarity between the two forms of representation of the model and gives strength to the use of the sphere representation in the modelling procedure in MOVIE. Figure 9(c) shows an end-on view of the best insect myosin filament model for eight crowns, also displayed as AVS. This nicely shows the overall arrangement of the outer heads with their motor domains projecting outwards and with the inner heads forming a ring round the backbone.

Another viewing mode is to show the model as a 3D electron density map so that we can easily compare it with myosin filament models from EM analysis. To do this, MOVIE can be run in the 'reflection mode' where it computes the Fourier transform of a model along with the phases in CCP13 or CCP4 type format. The CCP13 format output file can be loaded into LSQINT to simulate the diffraction pattern and then displayed with XFIX, making it easy to visually compare the calculated diffraction pattern with the observed pattern shown in figure 4(d). The CCP4 format output file can be used to create a 3D density map. A typical template file used in MOVIE to create an output ascii reflection file for the h, k, l, intensity values of the best model is shown in Figure 10(a). The resolution limit can be set and, for this particular example, it was put at 15 \AA resolution. The output file is then fed into a command file (Figure 10(b)) that runs various CCP4 programs to create the final 3D density map. The resolution of the reconstruction can be selected and for this particular example it was set at 200 \AA to 20 \AA . This map file is in CCP4 format. It can either be directly displayed in PYMOL or CHIMERA. However, if AVS is used to display the map file, then a field file is required by AVS to display the 3D density map produced by the command file of Figure 10(b). This field file is shown in Figure 10(c). The result is shown in Figure 11 where the best insect myosin filament model is visualised both in the sphere representation (Figure 11a) and as a 3D density map (Figure 11b:left).

Results for Insect Flight Muscle Myosin Filaments using the CCP13 and MOVIE programs

Application of MOVIE to the insect myosin filament diffraction data using the methods described above resulted in a best model with a 'goodness of fit' R-factor of 9.7% (AL-Khayat *et al.*, 2003). Interestingly, the best head conformation angles around

```

Terminal
MOVIE > status

Current Status

Modelling Method -
Global Parameter Search : DISABLED Down Hill Simplex Method : DISABLED
Powell's Method : DISABLED View Model : DISABLED
View Intensities : DISABLED Combined Refinement : DISABLED
Simulated Annealing : DISABLED Fourier Difference : DISABLED
Output Reflections : DISABLED Obs Output Reflections : DISABLED
Down Hill Replex Method : DISABLED Stochastic Torus Method : DISABLED

Similarity Measure -
Least Squares R-factor : DISABLED Similarity Weighting : DISABLED
Correlation Function : DISABLED Crystallographic R-factor: DISABLED
Scoring Method : DISABLED Manually Scale Data : DISABLED

Model Components -
Myosin Coordinates : DISABLED C_Protein Coordinates : DISABLED
Titin Coordinates : DISABLED Backbone Coordinates : DISABLED
Actin Coordinates : DISABLED Troponyosin Coordinates : DISABLED

Miscellaneous BOOL's -
OneShot Iteration : DISABLED Generate Bogus Data : DISABLED
BrookeHaven S1 : DISABLED No Perturbations : DISABLED

Search Range -

General Parameters -
No Of Molecular Strands : 0
Unit Cell Size : +0.0000A
Score Deviations : 0
Combine Weighting : 0.0
Number Of Filaments : 0
Resolution CutOff : 0.0
Total Repeat Of Model : +0.0000A
Intensity Filename :
Data Output Filename :

MOVIE > run
    
```

(a)

```

Template_sim_anneal.ini (modified)
This is a template file for use with Movie
Contained here is a set of commands
to initialize Movie properly for simulated annealing search

Hind AL-Khayat 14th July 2003

Myosin Parameters

myosin
noperts
besnum 20
myheads 2
MPCROWN 8
STRANDES 4
MREPEAT 1167.41
MRMASTER 14.29
MSPHERE 8.607
mpivpoint 21
CELL 523.44
NUMREPS 2
totrepeat 1167.41
replevel 10.66666667
FILAMENTS 1
cutoff 65.0
HEADFILE /usr/users/hind/programs/Movie/Head_Data/Myosin_14.29A_Rot_Trans.asc
IFILE /usr/users/hind/APSAUG99/h09blsqse1_msk.dat
mslew head 1 start -65.8027708024 scale 5.0
mtilt head 1 start 24.0833472556 scale 5.0
mrotation head 1 start 4.1338040059 scale 5.0
mslew head 2 start 37.7505657482 scale 5.0
mtilt head 2 start 30.8411207739 scale 5.0
mrotation head 2 start 44.1261372208 scale 5.0
mheadsep start 5.5099967394 scale 5.0
mheadang start -5.1702109525 scale 5.0
mradisc start 60.3245221391 scale 5.0
LATTICEROT START 292.3800154568 scale 5.0
mpivtilt start 0.5255349971 scale 5.0
mpivslew start 0.0329833660 scale 5.0
mpivrot start 5.0 scale 5.0
TEMPERATURE 0.3
TEMPDROP 0.9
ITERATIONS 3000
anneal leastsq weighted
OUTPUTFILE data_sim_anneal.dat
status
    
```

(b)

Figure 5. (a) Screen shot when initially running Movie with the default parameters, being zero for all model parameters and (b) a typical template file to run with MOVIE when using simulated annealing for global search.

```

Terminal
MOVIE > status

Current Status

Modelling Method -
Global Parameter Search : DISABLED Down Hill Simplex Method : DISABLED
Powell's Method : DISABLED View Model : DISABLED
View Intensities : DISABLED Combined Refinement : DISABLED
Simulated Annealing : ENABLED Fourier Difference : DISABLED
Output Reflections : DISABLED Obs Output Reflections : DISABLED
Down Hill Replex Method : DISABLED Stochastic Torus Method : DISABLED

Similarity Measure -
Least Squares R-factor : ENABLED Similarity Weighting : ENABLED
Correlation Function : DISABLED Crystallographic R-factor: DISABLED
Scoring Method : DISABLED Manually Scale Data : DISABLED

Model Components -
Myosin Coordinates : ENABLED C_Protein Coordinates : DISABLED
Titin Coordinates : DISABLED Backbone Coordinates : DISABLED
Actin Coordinates : DISABLED Troponyosin Coordinates : DISABLED

Miscellaneous BOOL's -
OneShot Iteration : ENABLED Generate Bogus Data : DISABLED
BrookeHaven S1 : DISABLED No Perturbations : ENABLED

Search Range -
Myosin Positional Parameters:
Rot Lat - +292.3800 to +292.3800 Step +0.0000 Scale +5.0000
Radius - +60.3245 to +60.3245 Step +0.0000 Scale +5.0000
Head Sep - +5.5100 to +5.5100 Step +0.0000 Scale +5.0000
Head Angle - -5.1702 to -5.1702 Step +0.0000 Scale +5.0000
Pivot Tilt - +0.5255 to +0.5255 Step +0.0000 Scale +5.0000
Pivot Slew - +0.0330 to +0.0330 Step +0.0000 Scale +5.0000
Pivot Rot - +5.0000 to +5.0000 Step +0.0000 Scale +5.0000

Head 1: Slew - -65.8028 to -65.8028 Step +0.0000 Scale +5.0000
Tilt - +24.0833 to +24.0833 Step +0.0000 Scale +5.0000
Rot - +4.1338 to +4.1338 Step +0.0000 Scale +5.0000
Head 2: Slew - -37.7506 to -37.7506 Step +0.0000 Scale +5.0000
Tilt - +30.8411 to +30.8411 Step +0.0000 Scale +5.0000
Rot - +44.1261 to +44.1261 Step +0.0000 Scale +5.0000
    
```

(a)

```

Terminal
Paxial - +0.0000 to +0.0000 Step +0.0000 Scale +0.0000
Pazimuthal - +0.0000 to +0.0000 Step +0.0000 Scale +0.0000
Level 4: PRad - +0.0000 to +0.0000 Step +0.0000 Scale +0.0000
Paxial - +0.0000 to +0.0000 Step +0.0000 Scale +0.0000
Pazimuthal - +0.0000 to +0.0000 Step +0.0000 Scale +0.0000
Level 5: PRad - +0.0000 to +0.0000 Step +0.0000 Scale +0.0000
Paxial - +0.0000 to +0.0000 Step +0.0000 Scale +0.0000
Pazimuthal - +0.0000 to +0.0000 Step +0.0000 Scale +0.0000
Level 6: PRad - +0.0000 to +0.0000 Step +0.0000 Scale +0.0000
Paxial - +0.0000 to +0.0000 Step +0.0000 Scale +0.0000
Pazimuthal - +0.0000 to +0.0000 Step +0.0000 Scale +0.0000
Level 7: PRad - +0.0000 to +0.0000 Step +0.0000 Scale +0.0000
Paxial - +0.0000 to +0.0000 Step +0.0000 Scale +0.0000
Pazimuthal - +0.0000 to +0.0000 Step +0.0000 Scale +0.0000
Level 8: PRad - +0.0000 to +0.0000 Step +0.0000 Scale +0.0000
Paxial - +0.0000 to +0.0000 Step +0.0000 Scale +0.0000
Pazimuthal - +0.0000 to +0.0000 Step +0.0000 Scale +0.0000

Myosin:
Myosin Repeat : +1167.4100A
Myosin Crowns per Repeat : 8
S1 Head Raster Size : 14.29A
S1 Head Sphere Size : 8.61A
S1 Head Filename : /usr/users/hind/programs/Movie/Head_Data/Myosin_14.29A_Rot_Trans.asc
Pivotal Sphere Number : 21
Number Of Myosin Heads : 2
Number of Turns In Repeat : 10.67

General Parameters -
No Of Molecular Strands : 4
Unit Cell Size : +523.4400A
Score Deviations : 0
Combine Weighting : 0.0
Number Of Filaments : 1
Resolution CutOff : 65.0
Number of Jn Functions : 20
Total Repeat Of Model : +1167.4100A
Intensity Filename : /usr/users/hind/APSAUG99/h09blsqse1_msk.dat
Data Output Filename : data_sim_anneal.dat
Temperature Factor : 0.300
Annealing Schedule : 3000
Temperature Drop Factor : +0.9000

MOVIE >
    
```

(b)

Figure 6. (a) Screen shot of the beginning and (b) the end of the output when using the template file in Figure 5(b).

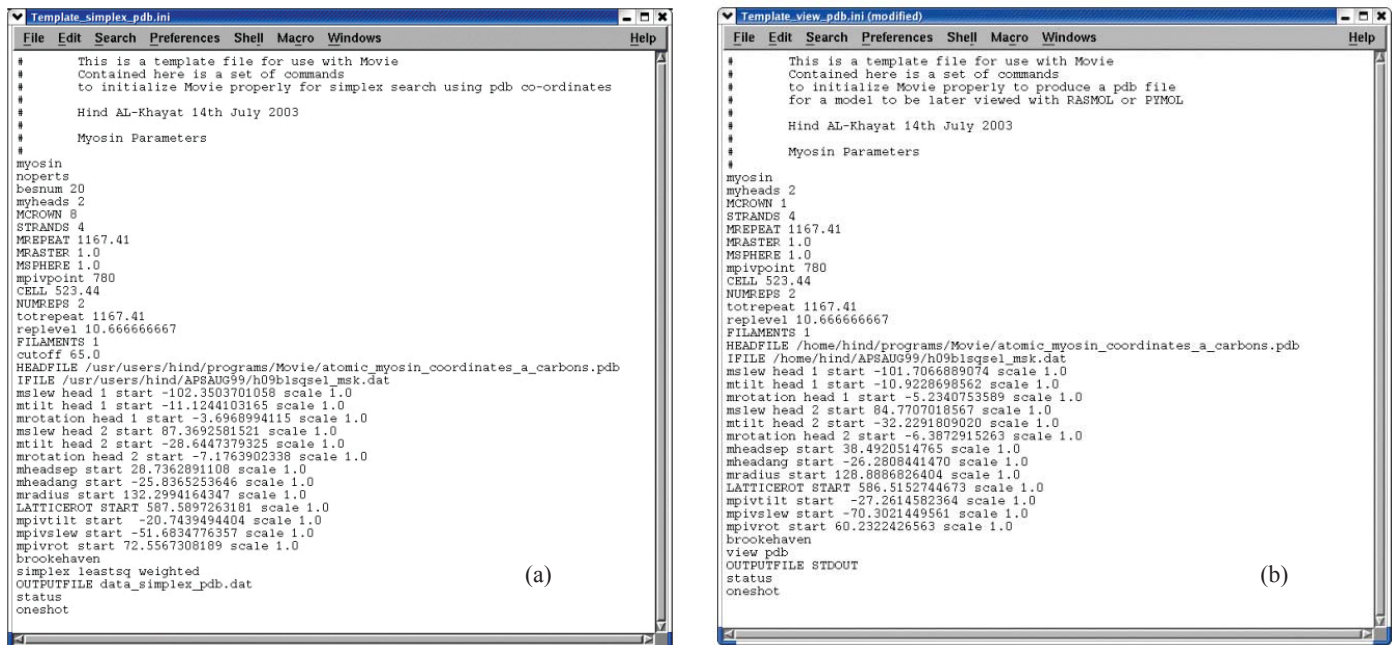


Figure 7. (a) Template file created to be used in MOVIE for a SIMPLEX search run for local minimisation and refinement. (b) Template file to be used in creating an output PDB file for the coordinates of a model.

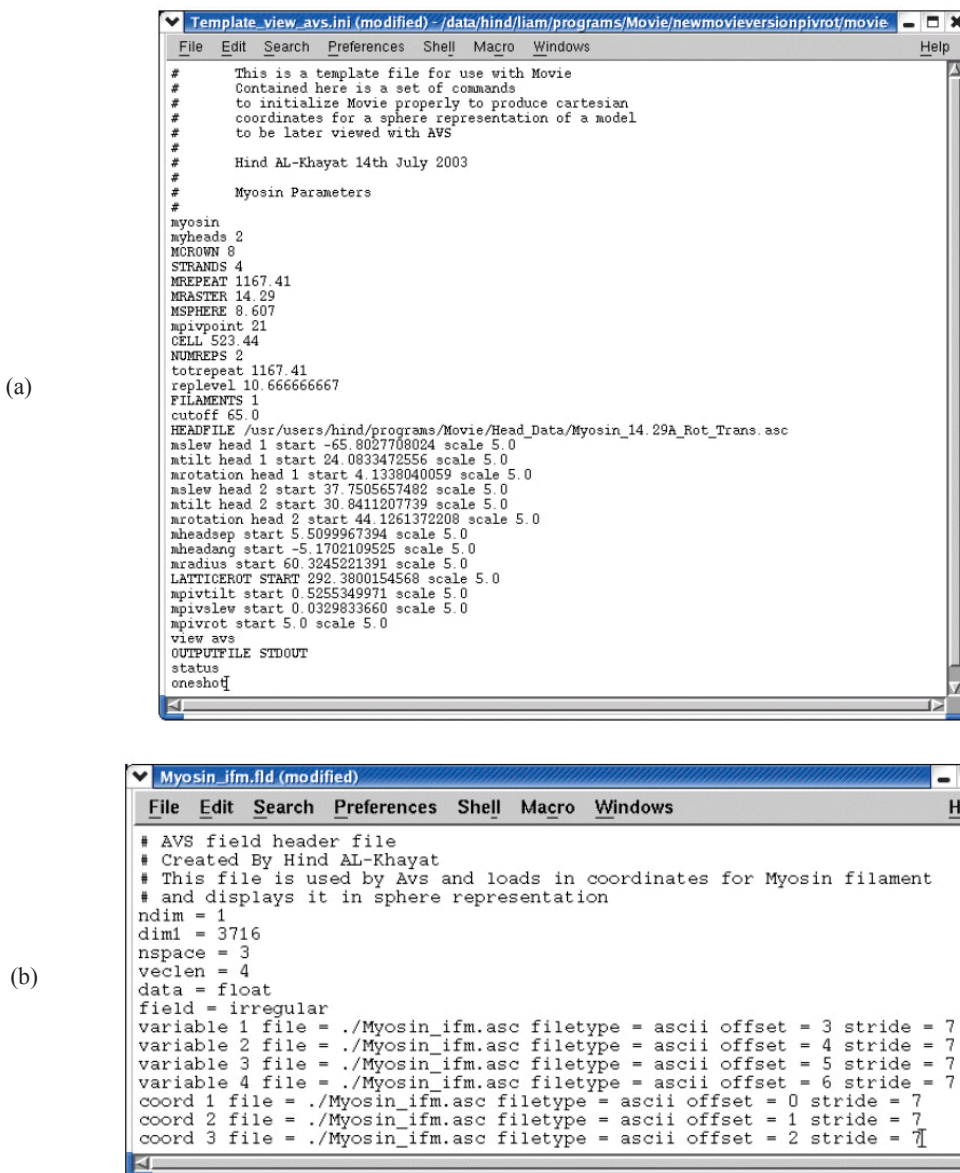


Figure 8. (a) Another form of output from MOVIE, outputting model parameter in cartesian coordinates for the positions of the centres of spheres and the radii of each, used in AVS for display, Template file to be used in creating an output ascii file for the cartesian coordinates of a sphere representation of the model. (b) field file required by AVS to display the sphere representation of a model produced in (a).

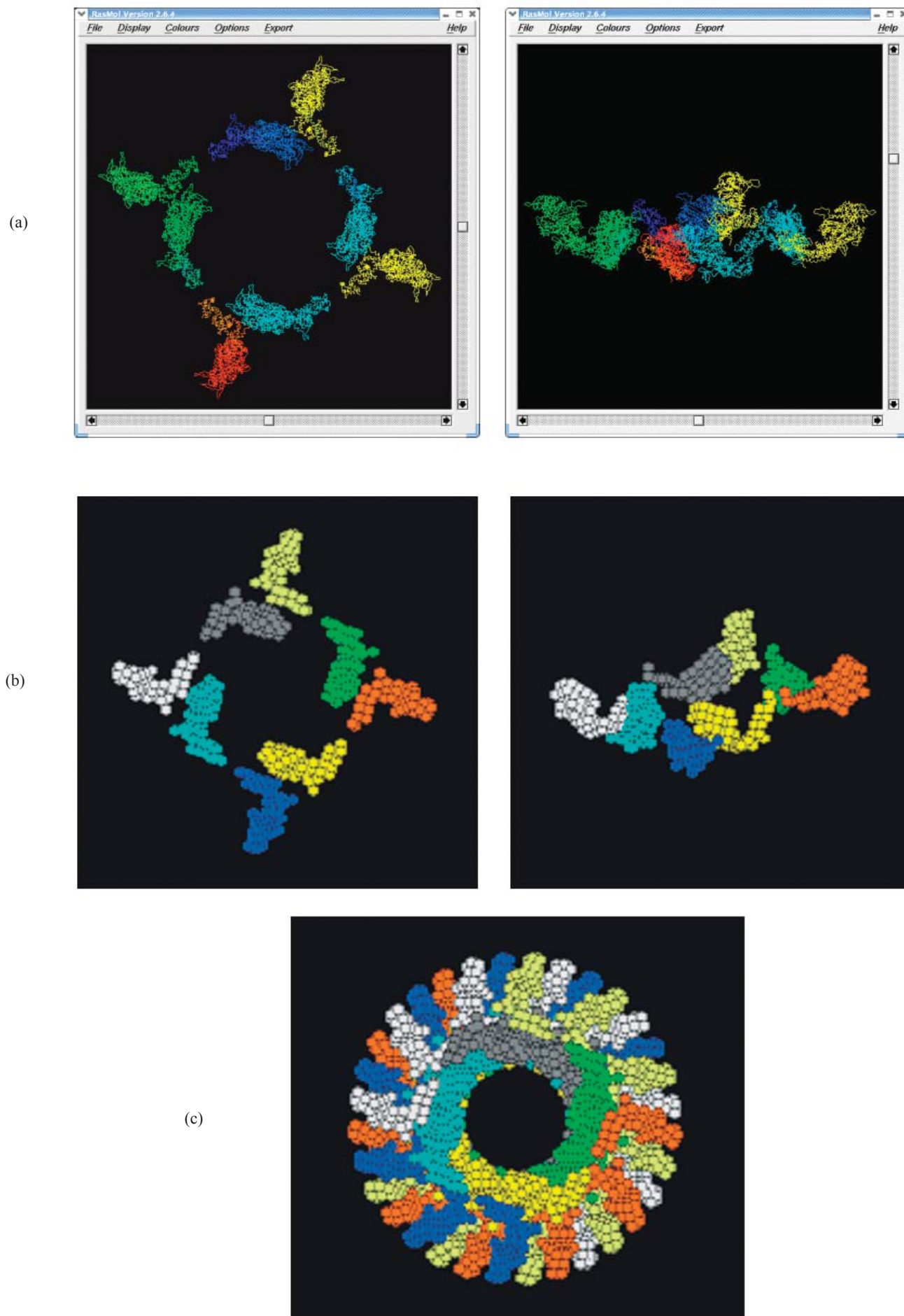


Figure 9. (a) MOVIE output as PDB coordinates and displayed in RASMOL, showing one crown in end-on view (left) and slightly tilted side view (right) for the best model. (b) same as in (a) but in the sphere representation, end-on view (left) and slightly tilted side view (right), for the best model displayed in AVS. (c) end-on view of the best model for eight crowns, also displayed in AVS.

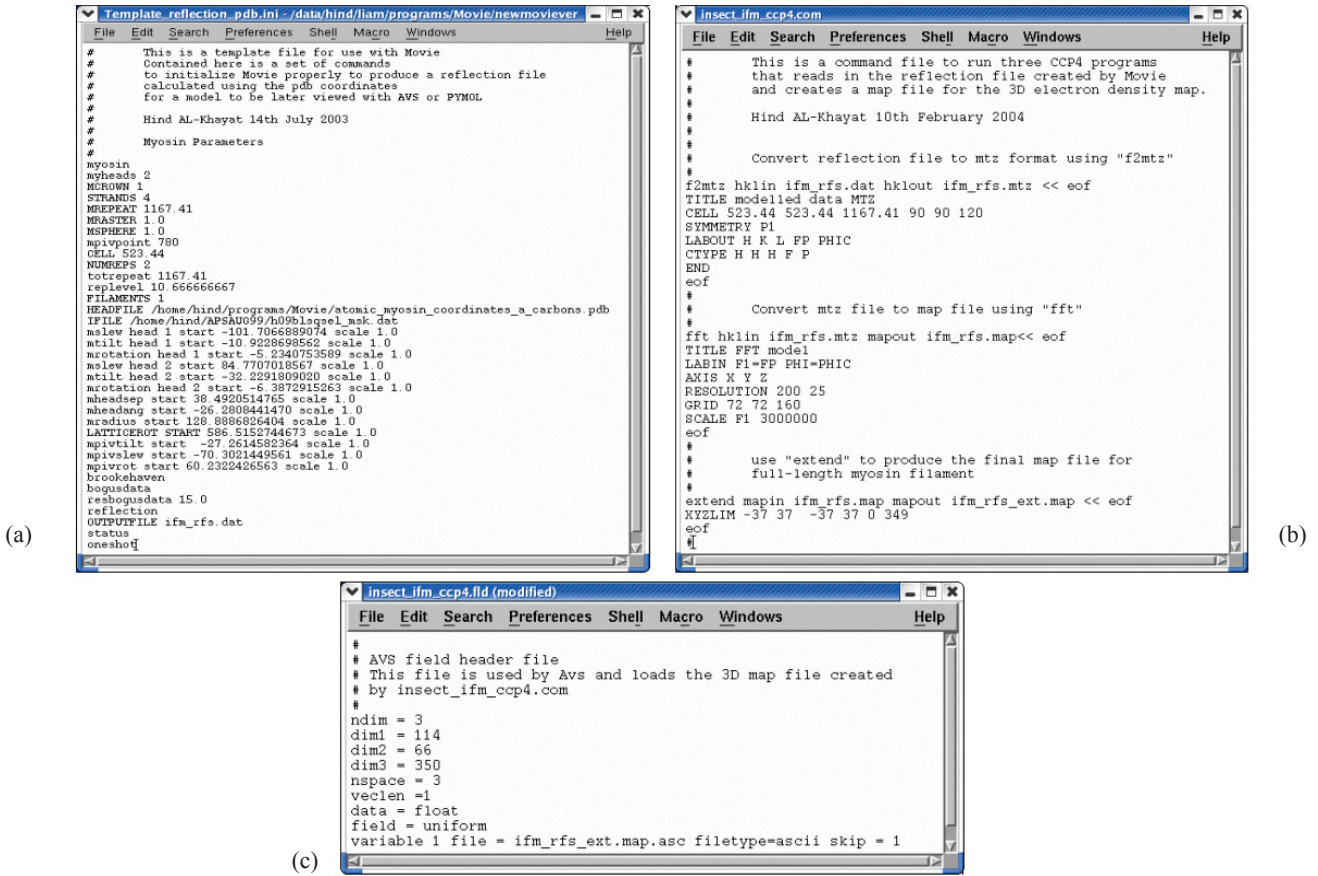


Figure 10. (a) Template file to be used in MOVIE to creating an output ascii reflection file for the h, k, l, intensity values of the best model. (b) command file that reads in the output file of (a) from MOVIE and uses various CCP4 programs to create a 3D density map. (c) field file required by AVS to display the 3D density map produced in (b).

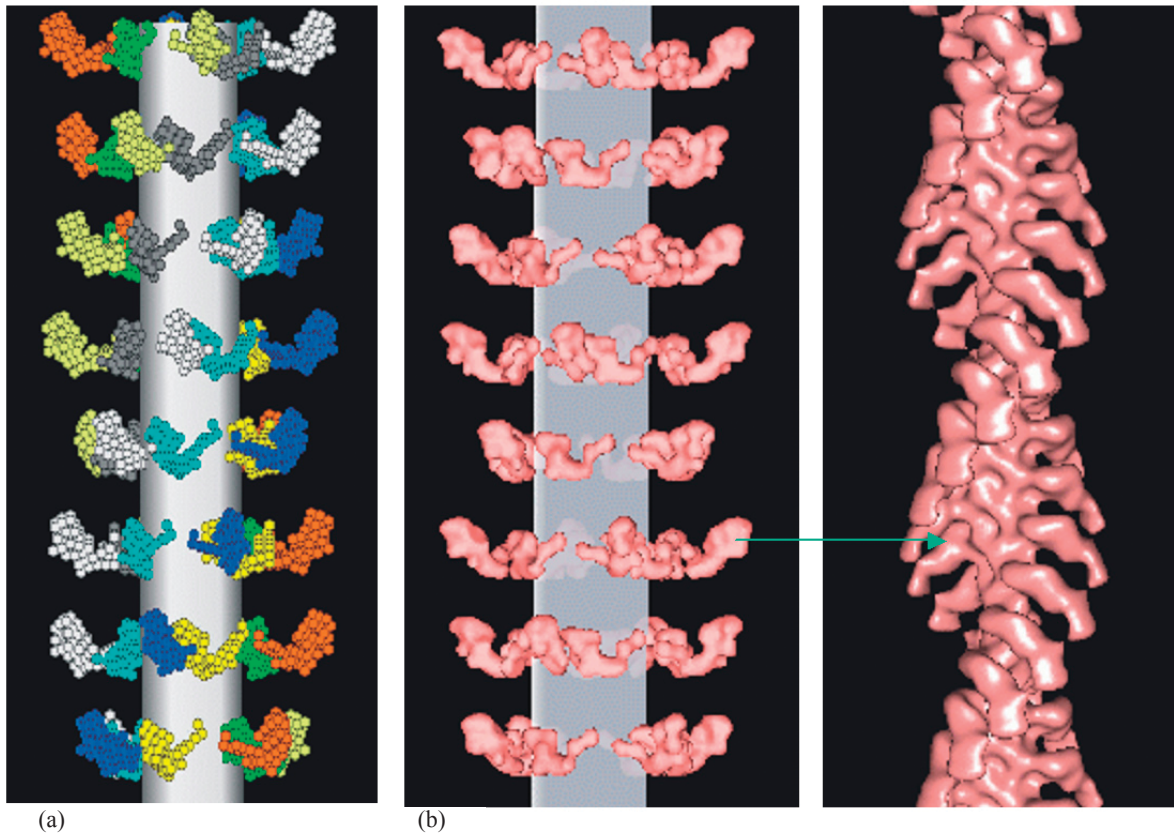


Figure 11. (a) The best model for IFM displayed as sphere representation, displayed in AVS. (b) left: as a 3-D density map using the PDB coordinates and reconstructed to 20 Å resolution, displayed in AVS; right: an actin filament labelled with S1 is shown to visualise the movement required by the myosin head in going from a relaxed myosin filament to finally attach to actin in the rigor confirmation, displayed in PYMOL.

the hinge gave a head shape that was close to that typical of relaxed M·ADP·Pi heads; a head shape never before demonstrated in intact muscle. The best packing constrained the 8 heads per crown within a compact crown shelf projecting perpendicular to the filament axis (Figure 11a, b:left). The two heads of each myosin molecule had non-equivalent positions, one head projecting outward while the other curves round the thick filament circumference to nose against the proximal neck of the projecting head of the neighbouring molecule (Figure 9a,b). The relaxed projecting head, oriented almost as needed for actin attachment, will attach, then release Pi followed by ADP, as the lever arm with a purely axial change in tilt drives ~100 Å of actin filament sliding on the way to the nucleotide-free limit of its working stroke (Figure 11b:right). ATP binding causes post-powerstroke myosin to release actin and relax again. Energy from splitting ATP fuels the next powerstroke. The four inward-pointing heads each touch an adjacent projecting head at a critical point, a contact that may simply inhibit the ability of both myosin heads to cleave high-energy ATP molecules. The final crown arrangement therefore appears well-designed to support the cycle of contraction of asynchronous fibrillar flight muscles used in flight by insects along with its well-known stretch-activation response. However, this is not the place to discuss such results in detail. This is done elsewhere (AL-Khayat *et al.*, 2003).

Our result shows that low-angle X-ray diffraction data is rich enough to give an atomic structure of the myosin head from intact relaxed muscle if used along with the powerful CCP13 stripping software and modelling by the simulated annealing search procedure using proteins of known molecular structures using MOVIE.

Potential of low-angle X-ray diffraction

The potential exists using this approach to fully 'solve' the whole of the resting *Lethocerus* flight muscle unit cell to 65 Å resolution or better. There is also data to higher resolution, both axially and radially, but the sampling might not be as good as in the low-angle pattern. However, this should be sufficient to enable us to model the full IFM unit cell, using all of the 468 independent observed reflections. The modelling should include all the unit cell protein components, including actin filaments, troponin and tropomyosin as well as the thick filament. Our results serve to illustrate that a great deal can be achieved with low-angle X-ray diffraction data given that it has been properly stripped (e.g. by the appropriate CCP13 software) and has been carefully modelled with proteins of known molecular structure and the appropriate modelling software (e.g. MOVIE). This analysis and previous modelling studies on actin filament structure using related methods (AL-Khayat *et al.*, 1995) confirm that highly accurate modelling with positional sensitivities of a few Å can be achieved from low-angle X-ray diffraction data.

In order to model the myosin pattern even better than has been done in the present study, we need to add more parameters for myosin. This includes allowing the two heads within a molecular pair to have different shapes as well non-equivalent positions. This will require the addition of three more parameters for the pivot slew, pivot tilt and pivot rotation of the second head and will be part of future efforts. Other minor protein components of the thick filament might also affect the

myosin intensities. It will be very interesting to study the contributions of these proteins to the low-angle diffraction pattern pattern, although it is assumed to be small, as was found in modelling the myosin filament structure of relaxed bony fish (Hudson *et al.*, 1997).

Conclusion

In summary, by rigorously stripping the low-angle X-ray diffraction pattern from relaxed insect flight muscle using CCP13 software and modelling the myosin filament structure using the program MOVIE we have been able to identify for the first time in intact muscle a myosin head shape clearly different from the nucleotide-free, rigor, state. This clearly illustrates the enormous power of the method. Our data add new and precise support for the active myosin head cycle first inferred from thin-section EM of relaxed and rigor IFM (Reedy *et al.*, 1965), finally showing resting cross-bridges truly at ~90°, with their actin-binding sites suitably oriented toward actin. The catalytic motor domain positions with respect to actin appear to be almost the same in both the relaxed and active or rigor states, as though the projecting relaxed heads are poised to enable very rapid attachment to correctly oriented target sites on an adjacent actin filament. Once the catalytic domain has attached, the head can sequentially release hydrolysis products Pi and ADP as it moves towards the nucleotide-free (rigor) state. This requires only an axial swing of the neck region (lever arm) through about 90° around the pivot point (making the whole head including the catalytic domain appear to rotate to the conventionally quoted 45° rigor angle) and giving an axial step of about 100 Å. An ATP-induced detachment and resetting of the head to the M·ADP·Pi state, followed by repositioning the head near to the original relaxed configuration will automatically set up another potential contractile cycle in the oscillating muscle. The resting myosin head configuration within the crown also provides a possible explanation for the uniquely developed stretch-activation response in insect flight muscle.

Acknowledgements

We thank Bruce Baumann for assistance in collecting fibre X-ray diffraction patterns from IFM at the Argonne/ APS/ BioCAT beamline. We acknowledge specific support for this work to JMS from a UK BBSRC project grant (# 28/S10891). MKR was supported by NIH AR-14317. CCP13 software was developed as part of UK BBSRC/ EPSRC funded projects (e.g. # 28/B10368 & 28/B15281). Use of the Advanced Photon Source was supported by the U.S. Department of Energy, Basic Energy Sciences, Office of Energy Research, under Contract No. W-31-109-ENG-38. BioCAT is a U.S. National Institutes of Health-supported Research Centre RR08630.

References

- [1] AL-Khayat, H.A., Yagi, N. & Squire, J.M. (1995) Structural changes in actin-tropomyosin during muscle regulation: Computer modelling low-angle X-ray diffraction data, *J. Molec. Biol.*, **252**, 611-632
- [2] AL-Khayat, H.A., Hudson, L., Reedy, M.K., Irving, T.C. & Squire, J.M. (2003) Myosin head configuration in relaxed

- insect flight muscle: X-ray modelled resting cross-bridges in a pre-powerstroke state are poised for actin binding, *Biophys. J.*, **85**, 1063-1079
- [3] Brent, R. P. (1973) *Algorithms for minimisation without derivatives* (Chap. 5) (Englewood Cliffs, NJ, Prentice-Hall).
- [4] Dominguez, R., Freyzon, Y., Trybus, K. M. & Cohen, C. (1998) Crystal structure of a vertebrate smooth muscle myosin motor domain and its complex with the essential light chain: visualization of the pre- power stroke state, *Cell*, **94**, 559-571
- [5] Harford, J. & Squire, J. M. (1997) Time-resolved diffraction studies of muscle using synchrotron radiation, *Rep. Prog. Phys.*, **60**, 1723-1787
- [6] Harford, J.J., Denny, R.C., Morris, E., Mendelson, R. & Squire, J.M. (1996) 3-D reconstruction from fibre X-ray diffraction patterns: Myosin-decorated actin filaments. *Fibre Diffraction Review*, **5**, 27-29.
- [7] Hibberd, M. G. & Trentham, D. R. (1986) Relationships between chemical and mechanical events during muscular contraction, *Ann. Rev. Biophys. & Biophys. Chem.*, **15**, 119-161
- [8] Houdusse, A., Szent-Gyorgyi, A. G. & Cohen, C. (2000) Three conformational states of scallop myosin S1, *Proc. Natl. Acad. Sci. U.S.A.*, **97**, 11238-11243
- [9] Hudson, L. (1996) *Ultrastructure of the A band unit cell in relaxed muscle*, Ph.D. thesis, University of London, London
- [10] Hudson, L., Harford, J. J., Denny, R. C. & Squire, J. M. (1997) Myosin head configuration in relaxed fish muscle: resting state myosin heads must swing axially by up to 150 Å or turn upside down to reach rigor, *J. Molec. Biol.*, **273**, 440-455
- [11] Irving, T. C., Fischetti, R., Rosenbaum, G. & Bunker, G. B. (2000) Fibre Diffraction Using the BioCAT Undulator Beamline at the Advanced Photon Source, *Nuclear Instruments and Methods (A)*, **448**, 250-254
- [12] Kirkpatrick, S., Gelatt, C. & Vecchi, M. (1983) Simulated annealing methods, *Science*, **220**, 671-680
- [13] Kirkpatrick, S. (1984) Simulated annealing methods, *J. Stat. Phys.*, **34**, 975-986
- [14] Nelder, J. & Mead, R. (1965) The simplex method for function minimisation, *Computer J.*, **7**, 308-313
- [15] Press, W. H., Teukolsky, S., Vetterling, T. and Flannery, B. (1992) *Numerical Recipes in C*, 2d edn (Cambridge, UK, Cambridge Univ. Press)
- [16] Rayment, I., Holden, H. M., Whittaker, M., Yohn, C. B., Lorenz, M., Holmes, K. C. & Milligan, R.A. (1993b) Structure of the actin-myosin complex and its implications for muscle contraction, *Science*, **261**, 58-65
- [17] Rayment, I., Rypniewsky, W. R., Schmidt-Bäse, K., Smith, R., Tomchick, D. R., Benning, M. M., Winkelmann, D. A., Wesenbergand, G. & Holden, H.M. (1993a) Three-dimensional structure of myosin subfragment-1: a molecular motor, *Science*, **261**, 50-58
- [18] Reedy, M. K., Holmes, K. C. & Tregear, R. T. (1965) Induced Changes in Orientation of the Cross-bridges of Glycerinated Insect Flight Muscle, *Nature*, **207**, 1276-1280
- [19] Reedy, M. K., Squire, J. M., Baumann, B. A., Stewart, A. & Irving, T. C. (2000) X-ray Fibre Diffraction of the Indirect Flight Muscle of *Lethocerus indicus*, In *Advanced Photon Source User Activity: Report 2000* (Argonne, IL, Argonne National Laboratory).
- [20] Squire, J. M. (2000) Fibre and Muscle Diffraction, In *Structure and Dynamics of Biomolecules*, E. Fanchon, E. Geissler, L.-L. Hodeau, J.-R. Regnard, and P. Timmins, eds. (Oxford, UK, Oxford Univ. Press), 272-301
- [21] Squire, J. M., Cantino, M., Chew, M., Denny, R., Harford, J., Hudson, L. and Luther, P. (1998) Myosin rod-packing schemes in vertebrate muscle thick filaments, *J. Struct. Biol.*, **122**, 128-138
- [22] Xu, S., Gu, J. Rhodes, T., Belknap, B., Rosenbaum, G., Offer, G., White H. & Yu., L.C. (1999) The M.ADP.P(i) state is required for helical order in the thick filaments of skeletal muscle, *Biophys. J.*, **77**, 2665-2676